Excellent passivation of germanium surfaces by POx/Al2O3 stacks

Applied Physics Letters

RESEARCH ARTICLE | AUGUST 30 2023

Excellent passivation of germanium surfaces by PO_x/Al_2O_3 stacks

Roel J. Theeuwes ; Wilhelmus J. H. Berghuis ; Bart Macco ; Wilhelmus M. M. Kessels

Appl. Phys. Lett. 123, 091604 (2023)
https://doi.org/10.1063/5.0164028

AIP Publishing

Applied Physics Letters ARTICLE pubs.aip.org/aip/apl

Excellent passivation of germanium surfaces by PO_x/Al_2O_3 stacks

Cite as: Appl. Phys. Lett. **123**, 091604 (2023); doi: 10.1063/5.0164028
Submitted: 20 June 2023 · Accepted: 16 August 2023 ·
Published Online: 30 August 2023

Roel J. Theeuwes,[a] Wilhelmus J. H. Berghuis, Bart Macco, and Wilhelmus M. M. Kessels[a]

AFFILIATIONS

Department of Applied Physics, Eindhoven University of Technology, P.O. Box 513, 5600 MB Eindhoven, The Netherlands

[a]Authors to whom correspondence should be addressed: r.j.theeuwes@tue.nl and w.m.m.kessels@tue.nl

ABSTRACT

Passivation of germanium surfaces is vital for the application of germanium in next-generation electronic and photonic devices. In this work, it is demonstrated that stacks of phosphorous oxide and aluminum oxide (PO_x/Al_2O_3) provide excellent and stable passivation of germanium surfaces, with state-of-the-art surface recombination velocities down to 8.9 cm/s. The PO_x/Al_2O_3 stack also exhibits positive fixed charge on germanium, which makes it especially suited for passivation of highly doped *n*-type germanium surfaces. The chemical passivation mechanism is found to be related to the passivation of defects by hydrogen, which is mobilized by the formation of $AlPO_4$ upon annealing. Furthermore, the GeO_x interlayer is removed due to a kind of "self-cleaning" process during the deposition of PO_x/Al_2O_3 stacks on germanium, which may in part explain the excellent passivation quality. This self-cleaning of the interface may also allow simplified device fabrication workflows, as pretreatments may be omitted.

Germanium is an attractive semiconductor for various emerging applications, due to its good optical properties and high charge carrier mobilities, and currently receives significant interest for logic applications,[1,2] quantum technologies,[3] photovoltaics,[4,5] and (infrared) photonics.[6,7] Although germanium is an indirect bandgap semiconductor (~0.66 eV),[8] strained germanium[9] and hexagonal germanium[10] were recently shown to exhibit direct bandgaps, which can enable efficient light emission. Moreover, germanium is highly compatible with silicon, which has led to germanium-on-silicon photonics,[11,12] and the use of silicon-germanium (SiGe) alloys in heterojunction bipolar transistors[13] and qubits.[14]

For many of these applications, defects at the germanium surface can significantly limit the device performance,[15,16] for example, through defect-assisted charge carrier recombination. The continued down-scaling of semiconductor and photonic devices, furthermore, leads to increased surface-to-volume ratios, which, in turn, leads to a more prominent role of these surface defects. To combat the detrimental effects of these defects, surface passivation can be employed, which is typically achieved by a reduction in the interface defect density (D_{it}), commonly known as chemical passivation. Additionally, surface recombination can be partially mitigated by a reduction in minority charge carriers at the interface, which is known as field-effect passivation. This can, for example, be achieved by a fixed charge density (Q_f) present at the interface or in the passivation layer.

Surface passivation of germanium has been a significant challenge,[17] which can be ascribed to the difficulty in forming a stable and high-quality interfacial layer on germanium. Recently, several passivation schemes on germanium have been investigated, many of which were inspired by silicon surface passivation, including Al_2O_3,[18,19] a-Si:H/Al_2O_3,[20] a-SiC_x/Al_2O_3,[21] SiN_x,[22,23] SiN_x/Al_2O_3,[22] and SiO_x/Al_2O_3.[24] This has resulted in varying levels of surface passivation with effective surface recombination velocities (S_{eff}) ranging between 1 and 200 cm/s. (Note these values are reported at various injection levels.) However, even with these recent additions, surface passivation of germanium remains challenging and effective passivation schemes for germanium remain scarce. Passivation schemes with positive Q_f on germanium are especially limited, which are particularly valuable for passivation of highly doped *n*-type germanium surfaces. It is noted that SiO_x and SiO_x/Al_2O_3 were identified to exhibit some positive Q_f on germanium,[24] while SiN_x—which has positive fixed charge on silicon—has negative fixed charge on germanium.[22,23]

Recently, stacks of phosphorus oxide and aluminum oxide (PO_x/Al_2O_3) have shown to lead to excellent surface passivation of silicon, which is enabled by a unique combination of very low D_{it} and high positive Q_f.[25–27] These PO_x/Al_2O_3 stacks were determined to have a

dielectric constant of 6.4 and a bandgap of >6 eV.[26] PO_x/Al_2O_3 has, furthermore, been shown to lead to effective surface passivation of indium phosphide,[28] where it also appeared to contain positive fixed charge.[29] In this Letter, we report excellent passivation of germanium surfaces by such PO_x/Al_2O_3 stacks. Furthermore, we investigate the mechanisms behind this passivation and compare it to surface passivation of germanium by Al_2O_3 and to surface passivation of silicon by PO_x/Al_2O_3 and Al_2O_3.

The PO_x/Al_2O_3 stacks were deposited symmetrically on 150 μm thick double-side polished 1–3 Ω cm *p*-type germanium (100) wafers and 280 μm double-side polished 1–5 Ω cm *n*-type silicon (100) wafers, using a deposition process based on chemical vapor deposition (CVD) and atomic layer deposition (ALD), which is described in detail in the supplementary material. The wafers received a 90 s 1% HF dip and were treated using a 1 min O_2 plasma prior to deposition of PO_x/Al_2O_3. The PO_x layer has a thickness of 5 nm and the Al_2O_3 layer has a thickness of 10 nm. Annealing was performed for 10 min in an N_2 ambient at various temperatures, similar to previous studies.[25,26] The surface passivation quality of PO_x/Al_2O_3 on germanium was assessed in the same fashion as on silicon, using quasi-steady-state photoconductance decay measurements.[30] These measurements were made suitable for germanium following the method described by Berghuis *et al.*,[19,31] which is also elaborately discussed by Martín *et al.*[32] The measurements were used to determine the minority carrier lifetimes ($\Delta n = 10^{15}$ cm^{-3}), from which the surface recombination velocity was calculated.

The surface recombination velocity (S_{eff}) for PO_x/Al_2O_3 and Al_2O_3 on germanium and silicon as a function of annealing temperature is shown in Fig. 1. The PO_x/Al_2O_3 stacks on germanium lead to excellent surface passivation, with a S_{eff} down to 9.5 cm/s after annealing at 250 °C. This is significantly better compared to Al_2O_3 on germanium, which leads to relatively high S_{eff} values (~10^3 cm/s). On silicon, both PO_x/Al_2O_3 and Al_2O_3 provide excellent surface passivation quality, indicated by the very low S_{eff} values (<10 cm/s). In Fig. 1, it can furthermore be seen that the optimal annealing temperatures for PO_x/Al_2O_3 on germanium and silicon are 250 and 350 °C, respectively. This difference in the optimal annealing temperature is notable, as for Al_2O_3 on germanium and silicon the optimal annealing temperature is quite similar (425 and 400 °C, respectively). For PO_x/Al_2O_3 on silicon, it was found that the chemical passivation mechanism is related to the passivation of silicon dangling bonds by hydrogen, which is mobilized by the formation of $AlPO_4$ upon annealing at 350 °C.[25,26] The chemical passivation mechanisms for PO_x/Al_2O_3 on germanium will be discussed below.

From Fig. 1, it is clear that there are differences between the passivation of germanium by PO_x/Al_2O_3 and Al_2O_3 and also between passivation of germanium and silicon by PO_x/Al_2O_3. To understand these differences and to understand the passivation of germanium by PO_x/Al_2O_3 stacks in general, several aspects of the PO_x/Al_2O_3 stacks on germanium have been investigated. This includes the presence of positive fixed charge, the chemical passivation mechanism, and the reduction and removal of the GeO_x by a kind of "self-cleaning" process during deposition of the PO_x/Al_2O_3 stacks. Furthermore, the stability of the surface passivation quality has been investigated, which is discussed first.

The stability of the surface passivation quality is presented in Fig. 2, where S_{eff} is shown as function of time for samples stored in ambient conditions in the dark. For PO_x/Al_2O_3 on germanium, the S_{eff} increased slightly from 8.9 to 14 cm/s in the first day, after which it stays constant at around 14 cm/s for more than 200 days, which suggests highly stable surface passivation. For Al_2O_3 on germanium, the S_{eff} decreased over time, and a significant drop in S_{eff} after around 30 days was observed.[19] After this drop, the S_{eff} stayed constant at around 300 cm/s. For PO_x/Al_2O_3 on silicon, an increase in S_{eff} could also be observed, but this increase is much slower than on germanium and starts only after 1 day. For Al_2O_3 on silicon, the passivation quality is very stable, and after around 1300 days even a very slight decrease in S_{eff} was observed. This is in line with earlier reports for stability of Al_2O_3 on silicon, where the passivation quality either stayed the same or improved slightly over time.[33]

For Al_2O_3 on germanium, the decrease in S_{eff} over time has been attributed to the generation of additional negative fixed charge.[20] For

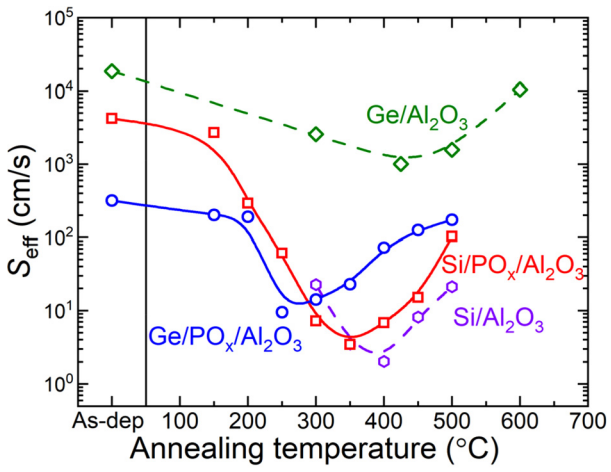

FIG. 1. Surface recombination velocity (S_{eff}) of germanium and silicon surfaces passivated by PO_x/Al_2O_3 as a function of annealing temperature. For reference, S_{eff} values for Al_2O_3 on germanium[19] and silicon[26] have also been added.

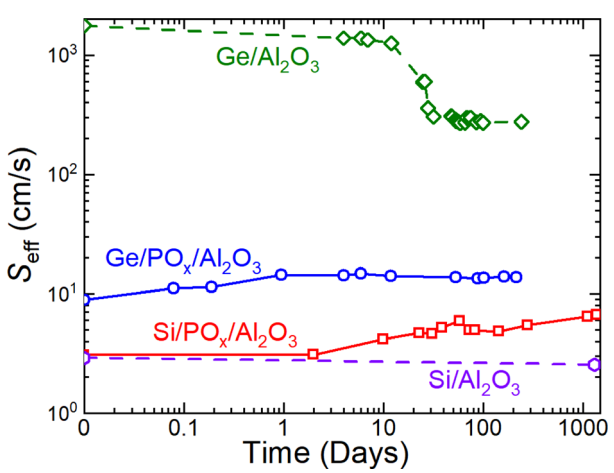

FIG. 2. S_{eff} of germanium and silicon surfaces passivated by PO_x/Al_2O_3 as a function of time. For reference, S_{eff} values for Al_2O_3 on germanium[19] and silicon have also been added.

Al_2O_3 on silicon, it was found that UV irradiation could lead to an increase in lifetime[33] (decrease in S_{eff}), which was also attributed to an increase in negative fixed charge density. The slight increase in the S_{eff} for silicon and germanium passivated by PO_x/Al_2O_3 might, therefore, also originate from a change in fixed charge density, which can, in particular, result from a slight decrease in positive Q_f.

To investigate whether the PO_x/Al_2O_3 stacks also provide positive fixed charge (Q_f) on germanium, the corona-lifetime method[25,34] has been employed. An increase in S_{eff} when depositing negative corona charges on the PO_x/Al_2O_3 was observed, as shown in Fig. 3. This indicates that the positive fixed charge in the dielectric is being compensated, which lowers the field-effect passivation. The deposition of net positive corona charge did not lead to an increase in S_{eff} of PO_x/Al_2O_3 on germanium as shown in the supplementary material, providing further evidence for the presence of positive fixed charge.

As opposed to corona-lifetime measurements for PO_x/Al_2O_3 on silicon, a peak in S_{eff} is not observed for PO_x/Al_2O_3 on germanium. Therefore, determination of the magnitude of Q_f is not possible. It is noted that the corona-lifetime method is not always non-intrusive, and the deposited corona charge density leads to relatively high electric fields across the measured dielectric, which could in some cases lead to charge injection.[23] It is possible that during the compensation of the positive fixed charge by the negative corona charges, more positive fixed charge is generated, and therefore, S_{eff} does not decrease again. This generation of more positive fixed charge for PO_x/Al_2O_3 on germanium may be facilitated by the absence of a GeO_x interlayer (as will be shown later), which means that the PO_x layer is in direct contact with the germanium semiconductor without a dielectric (tunneling) barrier.

Strikingly, it appears that the positive fixed charge of the PO_x/Al_2O_3 stacks is not influenced significantly by the underlying semiconductor, as the stack provides positive fixed charge on silicon, indium phosphide, and germanium. The presence of positive fixed charge on germanium is quite special, as even SiN_x—which has positive fixed charge on silicon—has a negative fixed charge on germanium.[22,23]

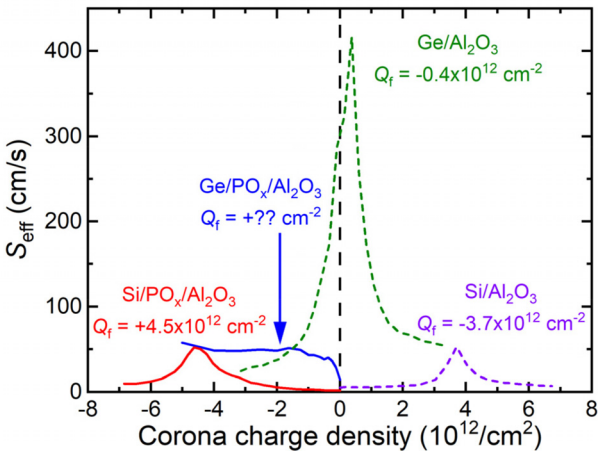

FIG. 3. S_{eff} as a function of corona charge density for PO_x/Al_2O_3 on Ge and Si.[27] For reference, corona charging curves of Al_2O_3 on Ge[23] and Si[23] are also added. The magnitude of Q_f can be determined from the corona charge density at the peak position of S_{eff} and has the opposite polarity. The magnitude of the positive Q_f could not be determined for PO_x/Al_2O_3 on germanium.

Infrared spectra of PO_x/Al_2O_3 stacks on silicon and germanium were determined for different annealing temperatures, as shown in Fig. 4. For PO_x/Al_2O_3 on silicon, the infrared spectra have been determined before[25,26] and correspond well to the current data. The peak assignments follow those determined previously.[25,26] The formation of the peak at 1100 cm^{-1} due to annealing is indicative of the formation of $AlPO_4$,[25,26] as this peak is characteristic for $[PO_4]^{3-}$ tetrahedra and is also a prominent absorption peak for $AlPO_4$ films. The formation of this peak is also observed on germanium, indicative of the formation of $AlPO_4$. Interestingly, the formation of this peak occurs at lower annealing temperature on germanium than on silicon, which is consistent with the shift in optimal annealing temperature, as observed in Fig. 1. On germanium, this peak is fully formed upon annealing at 250 °C, while on silicon the peak formation is completed at 350 °C. For annealing at higher temperatures up to 500 °C, there is no further increase in the intensity of this peak, as shown by the black line in Fig. 4.

On silicon, it was found that the chemical passivation mechanism of PO_x/Al_2O_3 is related to passivation of silicon dangling bonds by hydrogen, where the hydrogen is released by the formation of $AlPO_4$, which occurs at temperatures around 350–400 °C.[26] On germanium, the optimal annealing temperature and the temperature at which $AlPO_4$ is formed also coincide, but at a lower temperature of 250 °C. This suggests that PO_x/Al_2O_3 has a similar chemical passivation mechanism on germanium as on silicon, i.e., the formation of $AlPO_4$ leads to the release of hydrogen, which, in turn, leads to the passivation of dangling bonds and other defects at the semiconductor surface. The temperature at which this occurs appears to be affected by the underlying substrate. Based on previous observations on silicon,[26] it is expected that the field-effect passivation on germanium is not affected significantly by annealing. It is noted that hydrogen behaves differently in germanium and silicon,[15,35] and while it is expected that hydrogen can passivate defects on germanium, this is typically seen as being less effective on germanium as compared to silicon.[19,22,36]

The loss of hydrogen on both silicon and germanium at higher annealing temperatures can be identified by the lower absorbance in the 3000–3500 cm^{-1} region with increasing annealing temperatures, which are typically related to O–H vibrations.[37] This loss of hydrogen

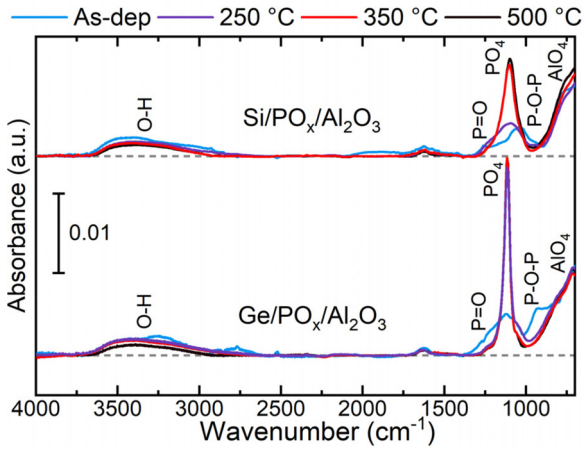

FIG. 4. Infrared spectra of as-deposited and annealed PO_x/Al_2O_3 stacks on Si and Ge.

can explain the depassivation—for example, by breaking of Si–H or Ge–H bonds—at higher annealing temperatures, as shown by the increase in S_{eff} in Fig. 1. The earlier onset of depassivation for PO_x/Al_2O_3 on germanium as compared to silicon may be in part related to the lower Ge–H (3.6 eV) bond energy with respect to the Si–H (3.9 eV) bond energy.[38]

X-ray photoelectron spectroscopy (XPS) depth profiles for as-deposited (solid line) and annealed (dashed line) PO_x/Al_2O_3 stacks on germanium are shown in Fig. 5(a). Note these XPS depth profiles are obtained using argon ion sputtering. As also observed previously on silicon,[25] aluminum is present in the PO_x layer already in the as deposited state. Upon annealing, there appear to be barely any changes to the XPS depth profiles, except for a slight change in the Al signal within the PO_x layer. This change in slope may be related to the formation of $AlPO_4$ (see Fig. 4) and was also observed for PO_x/Al_2O_3 on silicon. Note that the Al signal near the germanium surface is likely related to a sputter artifact.

In the XPS depth profiles, the presence of a GeO_x interlayer was not found for PO_x/Al_2O_3 on germanium. This is surprising, as the germanium surfaces were exposed to a 1 min O_2 plasma prior to deposition of the PO_x/Al_2O_3 stacks and a SiO_x interlayer is present for PO_x/Al_2O_3 on silicon. Therefore, it has been investigated how the deposition of the PO_x/Al_2O_3 stack affects the GeO_x interlayer. This is shown by the Ge3d spectra in Figs. 5(b)–5(d). The Ge3d spectra on the germanium wafer prior to deposition of the PO_x/Al_2O_3 stack are shown by the black solid lines for as-received GeO_x on *n*-type [Fig. 5(b)] and *p*-type [Fig. 5(c)] germanium and O_2-plasma grown (after HF dip) GeO_x on *p*-type germanium [Fig. 5(d)]. The last case is representative of the conditions used in the rest of this study. The Ge^{0+} ($3d_{5/2}$) and Ge^{4+} oxidation states are located at binding energies of 29.3 and 32.7 eV, respectively. In all cases, a GeO_x layer is clearly present as shown by the peak around 32.7 eV. The difference in relative peak height is likely related to different thicknesses of this initial GeO_x layer. The red solid line shows the Ge3d spectra after deposition of the PO_x/Al_2O_3 stacks, which are taken from depth profiles after 550 s of sputtering, i.e., at the PO_x/Ge interface, where the GeO_x layer should be present. After deposition of the PO_x/Al_2O_3 stacks, only a small GeO_x shoulder remains in Fig. 5(b), and no more GeO_x contributions can be observed in Figs. 5(c) and 5(d). These results indicate that the deposition of the PO_x/Al_2O_3 stacks lead to the reduction and removal of the GeO_x interlayer.

The reduction and removal of the GeO_x interlayer should be related to the PO_x layer, as the deposition of just Al_2O_3 on germanium results in a GeO_x interlayer.[19] The shoulder of GeO_x that remains after deposition of the PO_x/Al_2O_3 stack shown in Fig. 5(b) suggests that the PO_x is reducing the thickness of the GeO_x interlayer and was apparently not able to fully reduce/remove the GeO_x in this case. This might be because this GeO_x interlayer is thicker than those shown in Figs. 5(c) and 5(d).

This reduction and removal of the GeO_x interlayer resembles the interfacial "self-cleaning" of gallium arsenide by atomic layer deposition of Al_2O_3,[39] which is attributed to the interaction between the interfacial oxide and the precursor. However, the mechanism behind this "self-cleaning" process appears to be somewhat different in nature, as it was observed that a stack of 2 nm PO_x and 2 nm Al_2O_3 does not affect the GeO_x interlayer (not shown). This suggests that an interaction between the GeO_x and the PO_x precursor (trimethyl phosphate) at the start of the deposition is not simply responsible for the removal of the GeO_x. The current results suggest instead that the PO_x layer itself reduces the GeO_x interlayer thickness, with thin GeO_x layers even being fully removed. The exact mechanism behind this phenomenon requires additional investigation.

For surface passivation, interlayers can be highly important, and the SiO_x interlayer is often key for surface passivation of silicon. It is quite straightforward to obtain a high-quality SiO_x interlayer on silicon, while it is more challenging to form a high-quality GeO_x interlayer on germanium.[19,40] As shown in Fig. 1, PO_x/Al_2O_3 on germanium provides significantly better surface passivation than Al_2O_3 on germanium, which may be explained by this difference in GeO_x interlayer. The absence of the GeO_x interlayer for PO_x/Al_2O_3 on germanium suggests a Ge/PO_x interface, which may yield substantially lower interface defect density (D_{it}) as compared to the Ge/GeO_x interface for Al_2O_3 on germanium. This, in turn, can explain the lower S_{eff} for PO_x/Al_2O_3 on germanium, although the lack of a GeO_x layer may

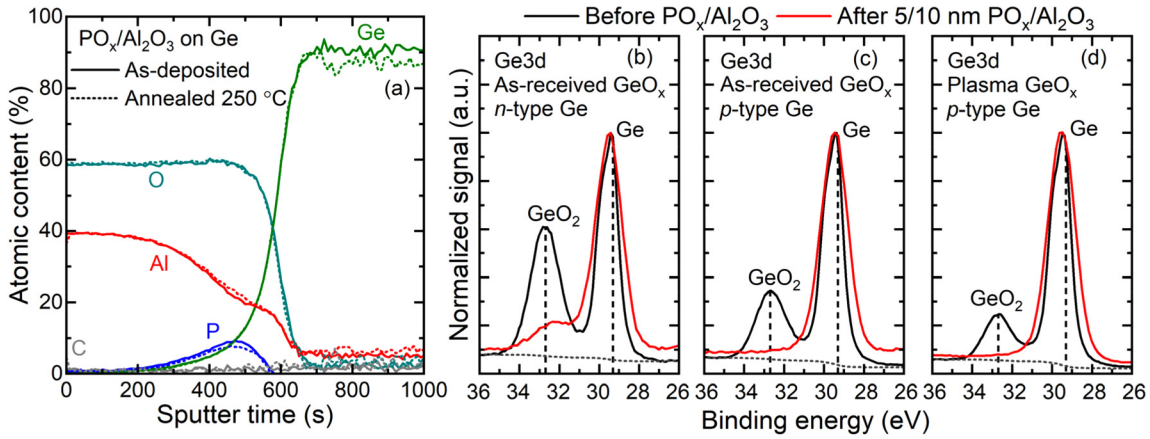

FIG. 5. (a) XPS depth profile for as-deposited and annealed PO_x/Al_2O_3 stacks on Ge (sputter time offset was used to align the germanium substrate). Normalized Ge3d spectra before and after PO_x/Al_2O_3 deposition on (b) as-received GeO_x on *n*-type germanium, (c) as-received GeO_x on *p*-type germanium, and (d) O_2-plasma grown GeO_x on *p*-type germanium. Ge3d peaks are charge referenced to elemental germanium.

also have some effect on the field-effect passivation. Furthermore, the removal of the GeO_x interlayer by the deposition process may also enable simplified device fabrication workflows, as pretreatments may be omitted.

In summary, the PO_x/Al_2O_3 stacks provide excellent and highly stable surface passivation quality on germanium, with S_{eff} values down to 8.9 cm/s. The PO_x/Al_2O_3 stack exhibits positive fixed charge on germanium and is, therefore, especially suited for the passivation of highly doped *n*-type germanium surfaces. The chemical passivation mechanism of PO_x/Al_2O_3 was found to be related to the passivation of surface defects by hydrogen, which is mobilized by the formation of $AlPO_4$ upon annealing. This process occurs already at 250 °C, which is lower than on silicon, suggesting an effect of the nature of the substrate on this process. The GeO_x interlayer is reduced and removed due to a sort of interfacial "self-cleaning" process upon deposition of PO_x/Al_2O_3 on germanium, which may in part explain the excellent surface passivation, and could allow simplified workflows for device fabrication. This investigation shows that PO_x/Al_2O_3 is a highly promising passivation scheme on germanium, and it contributes to the understanding of the passivation mechanisms. This understanding can be highly useful for the application of PO_x/Al_2O_3 stacks for surface passivation in next generation germanium-based electronic and photonic devices.

See the supplementary material for more details on the deposition processes and an additional corona-lifetime measurement of PO_x/Al_2O_3 on germanium.

This work was supported by The Netherlands Organization for Scientific Research (NWO) through the Gravitation/Zwaartekracht program "Research Centre for Integrated Nanophotonics" (Grant No. 024.002.033).

AUTHOR DECLARATIONS

Conflict of Interest

The authors have no conflicts to disclose.

Author Contributions

Roel J. Theeuwes: Conceptualization (equal); Investigation (equal); Methodology (equal); Writing – original draft (equal). **Wilhelmus (Willem-Jan) J. H. Berghuis:** Investigation (equal); Writing – review & editing (equal). **Bart Macco:** Supervision (equal); Writing – review & editing (equal). **W. M. M. Kessels:** Funding acquisition (equal); Supervision (equal); Writing – review & editing (equal).

DATA AVAILABILITY

The data that support the findings of this study are available from the corresponding authors upon reasonable request.

REFERENCES

[1]W. Rachmady, K. Jun, B. Krist, M. Metz, T. Michaelos, B. Mueller, A. A. Oni, R. Paul, A. Phan, P. Sears, T. Talukdar, A. Agrawal, J. Torres, R. Turkot, L. Wong, H. J. Yoo, J. Kavalieros, S. H. Sung, G. Dewey, S. Chouksey, B. Chu-Kung, G. Elbaz, P. Fischer, and C. Y. Huang, "300 mm heterogeneous 3D integration of record performance layer transfer germanium PMOS with silicon NMOS for low power high performance logic applications," in Technical Digest - International Electron Devices Meeting, IEDM 2019-December (2019).
[2]A. Toriumi and T. Nishimura, "Germanium CMOS potential from material and process perspectives: Be more positive about germanium," Jpn. J. Appl. Phys., Part 1 **57**(1), 010101 (2018).
[3]G. Scappucci, C. Kloeffel, F. A. Zwanenburg, D. Loss, M. Myronov, J. J. Zhang, S. De Franceschi, G. Katsaros, and M. Veldhorst, "The germanium quantum information route," Nat. Rev. Mater. **6**(10), 926–943 (2020).
[4]A. Alcañiz, G. López, I. Martín, A. Jiménez, A. Datas, E. Calle, E. Ros, L. G. Gerling, C. Voz, C. del Cañizo, and R. Alcubilla, "Germanium photovoltaic cells with MoOx hole-selective contacts," Sol. Energy **181**, 357–360 (2019).
[5]O. Hohn, G. Siefer, S. Janz, F. Dimroth, M. Niemeyer, C. Weiss, D. Lackner, F. Predan, A. Franke, P. Beutel, M. Schachtner, and R. Muller, "Development of germanium-based wafer-bonded four-junction solar cells," IEEE J. Photovoltaics **9**(6), 1625–1630 (2019).
[6]X. Zhang, J. Shao, S. Du, T. Lu, Y. Wang, F. Wang, Y. Geng, and Z. Tang, "Ultra-broadband, self-powered and high performance vertical $WSe_2/AlO_x/Ge$ heterojunction photodetector with MXene electrode," J. Alloys Compd. **930**, 167484 (2023).
[7]D. Marris-Morini, V. Vakarin, J. M. Ramirez, Q. Liu, A. Ballabio, J. Frigerio, M. Montesinos, C. Alonso-Ramos, X. Le Roux, S. Serna, D. Benedikovic, D. Chrastina, L. Vivien, and G. Isella, "Germanium-based integrated photonics from near- to mid-infrared applications," Nanophotonics **7**(11), 1781–1793 (2018).
[8]N. Mori, "Electronic band structures of silicon-germanium (SiGe) alloys," in *Silicon—Germanium (SiGe) Nanostructures: Production, Properties and Applications in Electronics*, edited by Y. Shiraki and N. Usami (Woodhead, 2011), pp. 26–42.
[9]F. T. Armand Pilon, A. Lyasota, Y. M. Niquet, V. Reboud, V. Calvo, N. Pauc, J. Widiez, C. Bonzon, J. M. Hartmann, A. Chelnokov, J. Faist, and H. Sigg, "Lasing in strained germanium microbridges," Nat. Commun. **10**(1), 2724 (2019).
[10]E. M. T. Fadaly, A. Dijkstra, J. R. Suckert, D. Ziss, M. A. J. van Tilburg, C. Mao, Y. Ren, V. T. van Lange, K. Korzun, S. Kölling, M. A. Verheijen, D. Busse, C. Rödl, J. Furthmüller, F. Bechstedt, J. Stangl, J. J. Finley, S. Botti, J. E. M. Haverkort, and E. P. A. M. Bakkers, "Direct-bandgap emission from hexagonal Ge and SiGe alloys," Nature **580**(7802), 205–209 (2020).
[11]J. Liu, "Monolithically integrated Ge-on-Si active photonics," Photonics **1**(3), 162–197 (2014).
[12]D. Benedikovic, L. Virot, G. Aubin, J. M. Hartmann, F. Amar, X. Le Roux, C. Alonso-Ramos, É. Cassan, D. Marris-Morini, J. M. Fédéli, F. Boeuf, B. Szelag, and L. Vivien, "Silicon-germanium receivers for short-wave-infrared optoelectronics and communications high-speed silicon-germanium receivers (invited review)," Nanophotonics **10**(3), 1059–1079 (2021).
[13]T. Zimmer, J. Bock, F. Buchali, P. Chevalier, M. Collisi, B. Debaillie, M. Deng, P. Ferrari, S. Fregonese, C. Gaquiere, H. Ghanem, H. Hettrich, A. Karakuzulu, T. Maiwald, M. Margalef-Rovira, C. Maye, M. Moller, A. Mukherjee, H. Rucker, P. Sakalas, R. Schmid, K. Schneider, K. Schuh, W. Templ, A. Visweswaran, and T. Zwick, "SiGe HBTs and BiCMOS technology for present and future millimeter-wave systems," IEEE J. Microwave **1**(1), 288–298 (2021).
[14]T. McJunkin, B. Harpt, Y. Feng, M. P. Losert, R. Rahman, J. P. Dodson, M. A. Wolfe, D. E. Savage, M. G. Lagally, S. N. Coppersmith, M. Friesen, R. Joynt, and M. A. Eriksson, "SiGe quantum wells with oscillating Ge concentrations for quantum dot qubits," Nat. Commun. **13**(1), 7777 (2022).
[15]J. R. Weber, A. Janotti, P. Rinke, and C. G. Van De Walle, "Dangling-bond defects and hydrogen passivation in germanium," Appl. Phys. Lett. **91**(14), 142101 (2007).
[16]N. E. Posthuma, G. Flamand, W. Geens, and J. Poortmans, "Surface passivation for germanium photovoltaic cells," Sol. Energy Mater. Sol. Cells **88**(1), 37–45 (2005).
[17]Q. Xie, S. Deng, M. Schaekers, D. Lin, M. Caymax, A. Delabie, X.-P. Qu, Y.-L. Jiang, D. Deduytsche, and C. Detavernier, "Germanium surface passivation and atomic layer deposition of high-*k* dielectrics—A tutorial review on Ge-based MOS capacitors," Semicond. Sci. Technol. **27**(7), 074012 (2012).
[18]J. Isometsä, T. H. Fung, T. P. Pasanen, H. Liu, M. Yli-Koski, V. Vähänissi, and H. Savin, "Achieving surface recombination velocity below 10 cm/s in n-type germanium using ALD Al_2O_3," APL Mater. **9**(11), 111113 (2021).

[19]W. J. H. Berghuis, J. Melskens, B. Macco, R. J. Theeuwes, M. A. Verheijen, and W. M. M. Kessels, "Surface passivation of germanium by atomic layer deposited Al_2O_3 nanolayers," J. Mater. Res. **36**(3), 571–581 (2021).
[20]W. J. H. Berghuis, J. Melskens, B. Macco, R. J. Theeuwes, L. E. Black, M. A. Verheijen, and W. M. M. Kessels, "Excellent surface passivation of germanium by a-Si:H/Al_2O_3 stacks," J. Appl. Phys. **130**(13), 135303 (2021).
[21]I. Martín, G. López, M. Garín, C. Voz, P. Ortega, and J. Puigdollers, "Effect of the thickness of amorphous silicon carbide interlayer on the passivation of c-Ge surface by aluminium oxide films," Surf. Interfaces **31**, 102070 (2022).
[22]H. Liu, T. P. Pasanen, T. H. Fung, J. Isometsä, O. Leiviskä, V. Vähänissi, and H. Savin, "Comparison of SiN_x-based surface passivation between germanium and silicon," Phys. Status Solidi A **220**(2), 2200690 (2023).
[23]W. J. H. Berghuis, M. Helmes, J. Melskens, R. J. Theeuwes, W. M. M. Kessels, and B. Macco, "Extracting surface recombination parameters of germanium–dielectric interfaces by corona-lifetime experiments," J. Appl. Phys. **131**(19), 195301 (2022).
[24]H. Liu, T. P. Pasanen, O. Leiviskä, J. Isometsä, T. H. Fung, M. Yli-Koski, M. Miettinen, P. Laukkanen, V. Vähänissi, and H. Savin, "Plasma-enhanced atomic layer deposited SiO_2 enables positive thin film charge and surface recombination velocity of 1.3 cm/s on germanium," Appl. Phys. Lett. **122**(19), 191602 (2023).
[25]R. J. Theeuwes, J. Melskens, L. E. Black, W. Beyer, D. Koushik, W. J. H. Berghuis, B. Macco, and W. M. M. Kessels, "PO_x/Al_2O_3 stacks for c-Si surface passivation: Material and interface properties," ACS Appl. Electron. Mater. **3**(10), 4337–4347 (2021).
[26]R. J. Theeuwes, J. Melskens, W. Beyer, U. Breuer, L. E. Black, W. J. H. Berghuis, B. Macco, and W. M. M. Kessels, "PO_x/Al_2O_3 stacks for surface passivation of Si and InP," Sol. Energy Mater. Sol. Cells **246**, 111911 (2022).
[27]J. Melskens, R. J. Theeuwes, L. E. Black, W. J. H. Berghuis, B. Macco, P. C. P. Bronsveld, and W. M. M. Kessels, "Excellent passivation of n-type silicon surfaces enabled by pulsed-flow plasma-enhanced chemical vapor deposition of phosphorus oxide capped by aluminum oxide," Phys. Status Solidi RRL **15**(1), 2000399 (2021).
[28]L. E. Black, A. Cavalli, M. A. Verheijen, J. E. M. Haverkort, E. P. A. M. Bakkers, and W. M. M. Kessels, "Effective surface passivation of InP nanowires by atomic-layer-deposited Al_2O_3 with PO_x interlayer," Nano Lett. **17**(10), 6287–6294 (2017).
[29]L. Hrachowina, X. Zou, Y. Chen, Y. Zhang, E. Barrigón, A. Yartsev, and M. T. Borgström, "Imaging the influence of oxides on the electrostatic potential of photovoltaic InP nanowires," Nano Res. **14**(11), 4087–4092 (2021).
[30]R. A. Sinton and A. Cuevas, "Contactless determination of current-voltage characteristics and minority-carrier lifetimes in semiconductors from quasi-steady-state photoconductance data," Appl. Phys. Lett. **69**(17), 2510–2512 (1996).
[31]W. J. H. Berghuis, "Nanolayers for germanium surface passivation prepared by atomic layer deposition and chemical vapor deposition," Ph.D. thesis (Eindhoven University of Technology, 2022).
[32]I. Martín, A. Alcaniz, A. Jimenez, G. Lopez, C. del Canizo, and A. Datas, "Application of quasi-steady-state photoconductance technique to lifetime measurements on crystalline germanium substrates," IEEE J. Photovoltaics **10**(4), 1068–1075 (2020).
[33]G. Dingemans, P. Engelhart, R. Seguin, F. Einsele, B. Hoex, M. C. M. van de Sanden, and W. M. M. Kessels, "Stability of Al_2O_3 and Al_2O_3/a-SiNx:H stacks for surface passivation of crystalline silicon," J. Appl. Phys. **106**(11), 114907 (2009).
[34]S. Dauwe, J. Schmidt, A. Metz, and R. Hezel, "Fixed charge density in silicon nitride films on crystalline silicon surfaces under illumination," in *Conference Record of the IEEE Photovoltaic Specialists Conference* (IEEE, 2002), pp. 162–165.
[35]A. Stesmans, T. Nguyen Hoang, and V. V. Afanas'Ev, "Hydrogen interaction kinetics of Ge dangling bonds at the $Si_{0.25}Ge_{0.75}/SiO_2$ interface," J. Appl. Phys. **116**(4), 044501 (2014).
[36]H. Matsubara, T. Sasada, M. Takenaka, and S. Takagi, "Evidence of low interface trap density in GeO_2/Ge metal-oxide-semiconductor structures fabricated by thermal oxidation," Appl. Phys. Lett. **93**(3), 032104 (2008).
[37]V. Verlaan, L. R. J. G. Van Den Elzen, G. Dingemans, M. C. M. Van De Sanden, and W. M. M. Kessels, "Composition and bonding structure of plasma-assisted ALD Al_2O_3 films," Phys. Status Solidi C **7**(3–4), 976–979 (2010).
[38]R. S. Grev, "Structure and bonding in the parent hydrides and multiply bonded silicon and germanium compounds: From Mh_n to $R_2M=M'R_2$ and $RM \equiv M'R$," Adv. Organomet. Chem. **33**(C), 125–170 (1991).
[39]C. L. Hinkle, A. M. Sonnet, E. M. Vogel, S. McDonnell, G. J. Hughes, M. Milojevic, B. Lee, F. S. Aguirre-Tostado, K. J. Choi, H. C. Kim, J. Kim, and R. M. Wallace, "GaAs interfacial self-cleaning by atomic layer deposition," Appl. Phys. Lett. **92**(7), 071901 (2008).
[40]J. Isometsä, Z. Jahanshah Rad, T. H. Fung, H. Liu, J. P. Lehtiö, T. P. Pasanen, O. Leiviskä, M. Miettinen, P. Laukkanen, K. Kokko, H. Savin, and V. Vähänissi, "Surface passivation of germanium with ALD Al_2O_3: Impact of composition and crystallinity of GeO_x interlayer," Crystals **13**(4), 667 (2023).